

Communication: Iteration-free, weighted histogram analysis method in terms of intensive variables

Jaegil Kim,^{a)} Thomas Keyes, and John E. Straub

Department of Chemistry, Boston University, Boston, Massachusetts 02215, USA

(Received 15 June 2011; accepted 28 July 2011; published online 11 August 2011)

We present an iteration-free weighted histogram method in terms of intensive variables that directly determines the inverse statistical temperature, $\beta_S = \partial S / \partial E$, with S the microcanonical entropy. The method eliminates iterative evaluations of the partition functions intrinsic to the conventional approach and leads to a dramatic acceleration of the posterior analysis of combining statistically independent simulations with no loss in accuracy. The synergistic combination of the method with generalized ensemble weights provides insights into the nature of the underlying phase transitions via signatures in β_S characteristic of finite size systems. The versatility and accuracy of the method is illustrated for the Ising and Potts models. © 2011 American Institute of Physics. [doi:10.1063/1.3626150]

The weighted histogram analysis method (WHAM) or multiple histogram method¹ is a powerful technique for combining multiple independent Monte Carlo (MC) or molecular dynamics simulations to consistently calculate thermodynamic properties. Enhanced sampling methods greatly benefit from WHAM, improving the precision of the density of states,² free energy differences,³ and potentials of mean force along reaction coordinates.⁴⁻⁷

The central quantity in the original formulation of WHAM (Ref. 1) is the density of states $\Omega(E)$ or the microcanonical entropy $S(E) = k_B \ln \Omega(E)$ ($k_B = 1$). In this approach, M independent simulations performed with the sampling weights $W_\alpha(E) = e^{-w_\alpha(E)}$ ($\alpha = 1, \dots, M$), and w_α the effective potential, are combined to determine the optimal estimate for Ω as

$$\tilde{\Omega}(E) = \frac{H(E)}{\sum_{\alpha=1}^M N_\alpha W_\alpha(E) / Z_\alpha}, \quad (1)$$

where $H(E) = \sum_\alpha H_\alpha$, $H_\alpha(E) = N_\alpha P_\alpha(E)$, and N_α and P_α are the number of samples and the normalized distribution in run α , respectively. The unknown relative partition function Z_α in Eq. (1) is determined self-consistently by solving $Z_\alpha = \sum_E \tilde{\Omega}(E, \{Z_{\alpha'}\}) W_\alpha$. The direct iteration method for Z_α is commonly used with the convergence criterion, $\sum_\alpha |(Z_\alpha^k - Z_\alpha^{k-1}) / Z_\alpha^k| \leq \delta_Z$, where δ_Z is a threshold value and k is the iteration step.² However, the convergence often becomes slow with increasing M , requiring thousands of iterations.⁸

In this paper, we propose an iteration-free, statistical temperature weighted histogram analysis method (ST-WHAM). While conventional WHAM is formulated in terms of all extensive quantities $\{S; H_\alpha, W_\alpha\}$, ST-WHAM is expressed in terms of the corresponding derivatives. The goal is to directly determine the inverse statistical temperature $\beta_S = \partial S / \partial E$ as a weighted superposition of the individual statistical tempera-

ture estimates, $\beta_\alpha^S = \partial \ln H_\alpha / \partial E - \partial \ln W_\alpha / \partial E$, with no undetermined parameters. Eliminating the need to determine Z_α leads to a substantial acceleration of the posterior analysis of merging independent runs without a loss in accuracy. The determination of β_S yields S , and reveals valuable information characteristic of phase transitions in finite size systems.⁹

Basic formulation: We proceed by first converting Eq. (1) into a weighted average of the individual density of states estimates, $\Omega_\alpha = H_\alpha / \Pi_\alpha$, $\Pi_\alpha = N_\alpha W_\alpha / Z_\alpha$,

$$\tilde{\Omega}(E) = \sum_\alpha \tilde{f}_\alpha(E) \Omega_\alpha(E), \quad (2)$$

where \tilde{f}_α represents the energy-dependent, normalized weight, $\Pi_\alpha / \sum_\alpha \Pi_\alpha$. Multiplying the numerator and denominator by $\tilde{\Omega}$ further identifies $\tilde{f}_\alpha = \tilde{H}_\alpha / H$, where the histogram $\tilde{H}_\alpha = \tilde{\Omega} \Pi_\alpha$ is reweighted by $\tilde{\Omega}$. The reweighted \tilde{H}_α is not necessarily identical to the simulated H_α even though $\sum_\alpha \tilde{H}_\alpha = H$ and $\sum_E \tilde{H}_\alpha = N_\alpha$.

We take the logarithm of both sides of Eq. (2) and differentiate with respect to E to express

$$\tilde{\beta}_S = \frac{\partial \ln \tilde{\Omega}}{\partial E} = \sum_\alpha f_\alpha^* \frac{\partial \ln \Omega_\alpha}{\partial E} + \sum_\alpha f_\alpha^* \frac{\partial \ln \tilde{f}_\alpha}{\partial E}, \quad (3)$$

where $f_\alpha^* = (\Omega_\alpha / \tilde{\Omega}) \tilde{f}_\alpha = H_\alpha / H$ is the simulated histogram fraction. Throughout the paper the “*” symbol denotes ST-WHAM estimates.

The first term in Eq. (3) is a weighted superposition of each individual statistical temperature estimate, $\beta_\alpha^S = \partial \ln H_\alpha / \partial E - \partial \ln W_\alpha / \partial E$, yielding the ST-WHAM estimate for β_S , as

$$\beta_S^* = \sum_\alpha f_\alpha^* (\beta_\alpha^H + \beta_\alpha^{\text{eff}}) = \beta_H + \beta_W, \quad (4)$$

where $\beta_H = \sum_\alpha f_\alpha^* \beta_\alpha^H$, $\beta_\alpha^H = \partial \ln H_\alpha / \partial E$, and $\beta_W = \sum_\alpha f_\alpha^* \beta_\alpha^{\text{eff}}$, with $\beta_\alpha^{\text{eff}} = \partial w_\alpha / \partial E$ the weight-dependent, inverse effective temperature.¹⁰ The key observation is that with no undetermined parameters, Eq. (4) uniquely determines β_S^* by weighting the known, intensive

^{a)}Electronic mail: jaegilkim89@gmail.com. Present address: Broad Institute of MIT and Harvard, Cambridge, MA 02142, USA.

estimates, β_α^H and $\beta_\alpha^{\text{eff}}$, in proportion to the number of samples in the corresponding histograms at energy E . In contrast, smoothly joining the extensive quantity Ω_α requires the determination of Z_α , even though \tilde{f}_α is replaced by f_α^* in Eq. (2).

The second term in Eq. (3) is the difference between the WHAM and ST-WHAM estimates, and after substituting \tilde{f}_α reduces to

$$\delta\beta_S = \tilde{\beta}_S - \beta_S^* = \sum_\alpha f_\alpha^* (\beta_\alpha^{\tilde{H}} - \beta_\alpha^H), \quad (5)$$

yielding $\tilde{\beta}_S = \sum_\alpha f_\alpha^* (\beta_\alpha^{\tilde{H}} + \beta_\alpha^{\text{eff}})$. Note that with replacing \tilde{H}_α by H_α , $\tilde{\beta}_S$ leads to β_S^* and $\delta\beta_S \simeq \sum_\alpha f_\alpha^* \partial \ln f_\alpha^* / \partial E = \partial \sum_\alpha f_\alpha^* / \partial E = 0$. As N_α increases, both \tilde{H}_α and H_α rapidly converge to the exact result $H_\alpha^{\text{ex}} = N_\alpha P_\alpha^{\text{ex}}$, where “ex” denotes exact values. Hence, the accuracy of both methods is similar with $\delta\beta_S \simeq 0$ for $N_\alpha \gg 1$, which we will demonstrate for the Ising model.

Once β_S^* is determined via Eq. (4) we can compute the corresponding entropy estimate

$$S^* = \sum_\alpha \int_{E_L}^E f_\alpha^*(z) \beta_\alpha^S(z) dz = \sum_\alpha \int_{E_L}^E \tilde{\beta}_\alpha^S(z) dz, \quad (6)$$

where $\tilde{\beta}_\alpha^S = \tilde{\beta}_\alpha^H - \tilde{\beta}_\alpha^W$, $\tilde{A} = f_\alpha^* \mathcal{A}$. Directly integrating Eq. (6) is not desirable due to the rapid variation of β_S for small E . We approximate the statistical temperature $T_S^* = \beta_S^{*-1}$ on an equally spaced energy grid $E_j = G(E/\Delta)\Delta$, where Δ is the bin size and $G(x)$ returns the nearest integer to x . Hence, $T_S^*(E) \simeq T_j^* + \eta_j(E - E_j)$ for $E \in [E_j, E_{j+1}]$, with $T_j^* = T_S^*(E_j)$ and $\eta_j = (T_{j+1}^* - T_j^*)/\Delta$. This approximation allows an analytical integration and gives a mapping from β_S^* to

$$S^* = \sum_{j=L}^{i_{\max}} L_j(E_{j+1}) + L_{i_{\max}}(E), \quad (7)$$

where $L_j = 1/\eta_j \ln[1 + \eta_j(E - E_j)/T_j^*]$, and $i_{\max} = i - 1$ if $E \in [E_i - \Delta/2, E_i]$, and $i_{\max} = i$ if $E \in [E_i, E_i + \Delta/2]$.

The same strategy is equally applicable to the potential mean force (PMF) calculation along the reaction coordinate $\eta(\mathbf{x})$, \mathbf{x} being coordinates. The PMF at the inverse temperature β_0 with the reference potential w_0 is determined as $-\frac{1}{\beta_0} \ln \rho(\eta)$, $\rho(\eta) = \int d\mathbf{x} \delta[\eta(\mathbf{x}) - \eta] W_0(\mathbf{x}) / Z_0$, $W_0 = e^{-\beta_0 w_0}$. The WHAM estimate for $\rho(\eta)$, conjugated with multiple runs with the sampling weight $W_\alpha = \exp\{-\beta_0(w_0 + w_\alpha(\eta))\}$, w_α being the biasing potential, is obtained⁵ as

$$\tilde{\rho}(\eta) = \frac{H(\eta)}{\sum_{\alpha=1}^M N_\alpha \tilde{W}_\alpha(\eta) / Z_\alpha}, \quad (8)$$

$\tilde{W}_\alpha = \exp\{-\beta_0 w_\alpha\}$. Denoting each individual estimate, $\rho_\alpha = H_\alpha / \Pi_\alpha$, $\Pi_\alpha = N_\alpha \tilde{W}_\alpha / Z_\alpha$, Eq. (8) further transforms to

$$\tilde{\rho}(\eta) = \sum_\alpha \tilde{f}_\alpha(\eta) \rho_\alpha(\eta) \quad (9)$$

analogous to Eq. (2). Taking the logarithm of both sides and differentiating with respect to η yields the WHAM estimate

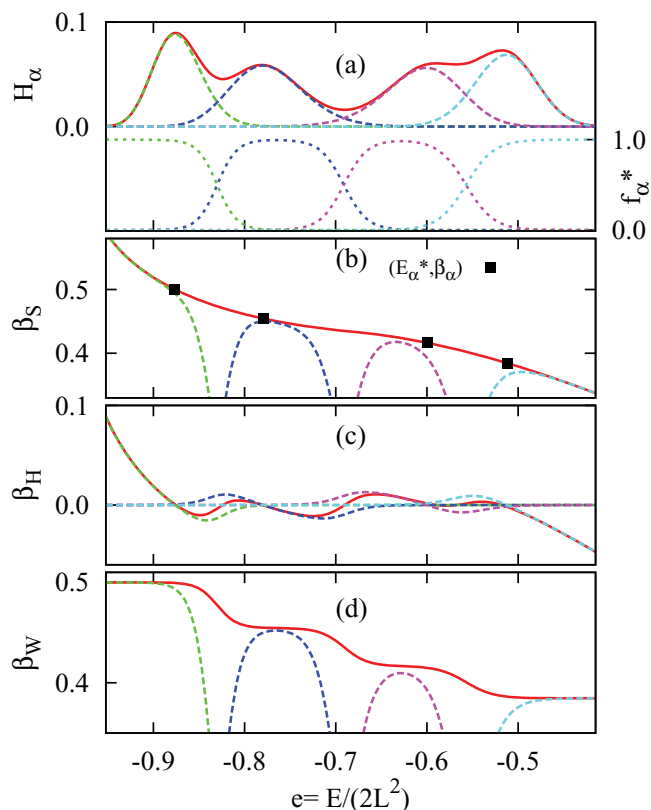


FIG. 1. ST-WHAM results for the 2D Ising model with linear dimension $L = 32$ and $M = 4$. (a) H_α^{ex} (solid line), H_α^{ex} (dashed line), and $f_\alpha^* = H_\alpha^{\text{ex}}/H_\alpha^{\text{ex}}$ (dotted line); (b) β_S^* (solid line) and $\tilde{\beta}_S^*$ (dashed line); (c) β_H (solid line) and $\tilde{\beta}_H^*$ (dashed line), and (d) β_W (solid line) and $\tilde{\beta}_W^*$ (dashed line) as a function of $e = E/2L^2$. The magnitude of H_α^{ex} is adjusted for visualization, and $\alpha = 1, 2, 3,$ and 4 from left to right in (a). The same color scheme is used for all figures.

for the derivative of $\ln \rho(\eta)$ as

$$\frac{\partial \ln \tilde{\rho}}{\partial \eta} = \sum_\alpha f_\alpha^* \left[\frac{\partial \ln H_\alpha}{\partial \eta} + \beta_0 \frac{\partial w_\alpha}{\partial \eta} \right] + \sum_\alpha f_\alpha^* \frac{\partial \ln \tilde{f}_\alpha}{\partial \eta}. \quad (10)$$

By retaining only the first term in Eq. (10) the ST-WHAM estimate for $\frac{\partial \ln \rho}{\partial \eta}$ is obtained as a weighted superposition of $\partial \ln \rho_\alpha / \partial \eta$ over the simulated histogram fraction f_α^* as in Eq. (4). A similar expression to the first term in Eq. (10) is also derived in the “umbrella integration” by extending the thermodynamic integration method and has shown to reduce the statistical errors compared to conventional WHAM.⁶

Numerical simulations: The determination of β_S^* by ST-WHAM given H_α and W_α is now illustrated for the 2D Ising model. We exploit the known exact values S^{ex} (Ref. 11) to prepare the normalized histograms, $H_{\alpha,i}^{\text{ex}} = \exp\{S_i^{\text{ex}} - E_i/T_\alpha\} / (\Delta \sum_i \exp\{S_i^{\text{ex}} - E_i/T_\alpha\})$, with $\Delta = 4$ at four equally distributed temperatures T_α between $T_1 = 2.0$ and $T_4 = 2.6$ [see Fig. 1(a)]. The normalized weight f_α^* in Fig. 1(a) equals one for non-overlapping energy regions and rapidly decreases to zero as H_α^{ex} decreases.

By replacing $\beta_\alpha^H(E_i)$ by its finite difference form, $\ln(H_{\alpha,i+1}^{\text{ex}}/H_{\alpha,i-1}^{\text{ex}})/(2\Delta)$, Eq. (4) determines the smoothly varying β_S^* in Fig. 1(b), which is indistinguishable from $\beta_S^{\text{ex}} = (S_{i+1}^{\text{ex}} - S_{i-1}^{\text{ex}})/(2\Delta)$. Both $\tilde{\beta}_\alpha^H$ and $\tilde{\beta}_\alpha^W$ in Figs. 1(c) and

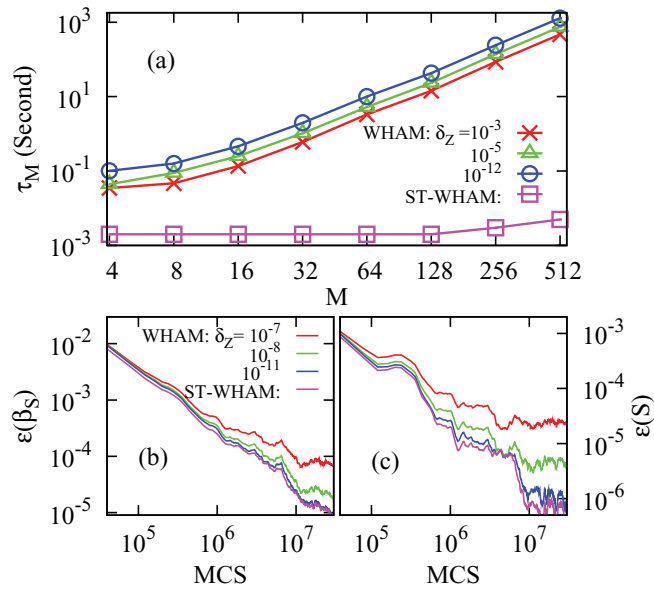


FIG. 2. (a) Time τ_M required to compute S given H_α^{ex} at M equally distributed temperatures between $T_1 = 2.0$ and $T_M = 2.6$ for $L = 32$, (b) the error estimates $\epsilon(\beta_S)$, and (c) $\epsilon(S)$ as a function of Monte Carlo steps per spin (MCS) averaged over ten realizations of canonical runs with $M = 4$.

1(d), respectively, are significant only for $f_\alpha^* \neq 0$. Approximating $H_\alpha^{\text{ex}} \approx \exp[\beta'_S(E_\alpha^*)(E - E_\alpha^*)^2/2]$, where the prime indicates differentiation and E_α^* is determined from $\beta_S(E_\alpha^*) = \beta_\alpha$, we find that $\beta_\alpha^H \approx \beta'_S(E_\alpha^*)(E - E_\alpha^*)$ changes sign as E crosses E_α^* , giving rise to the oscillatory behavior of β_H in Fig. 1(c). The weighted average of $\beta_W = \sum_\alpha f_\alpha^* \beta_\alpha^{\text{eff}}$, $\beta_\alpha^{\text{eff}} = \beta_\alpha$, exhibits a staircase modulation [see Fig. 1(d)] and offsets β_H , resulting in $\beta_S^* \approx \sum_\alpha f_\alpha^* [\beta'_S(E_\alpha^*)(E - E_\alpha^*) + \beta_\alpha]$ corresponding to a weighted superposition of tangents of β_S at E_α^* .

As $\beta_S^* \simeq \beta_S^{\text{ex}}$ most errors in S^* arise from the mapping in Eq. (7). To examine the accuracy of this mapping we compute the error $\epsilon(S^*)$, with $\epsilon(A) = \sum_i |(A_i - A_i^{\text{ex}})/A_i^{\text{ex}}|^2$ for $E_i \in [E_1^*, E_M^*]$, by shifting S_i^* and S_i^{ex} to their corresponding values at E_1^* . We find $\epsilon(S^*) \approx 10^{-9}$, showing that the error is negligible, even though the energies are discrete. To demonstrate the speed-up of the posterior data analysis using ST-WHAM we compare the time, τ_M , needed to determine the entropy estimate for increasing M . Histograms H_α^{ex} ($\alpha = 1, \dots, M$) are prepared at M equally divided temperatures between $T_1 = 2.0$ and $T_M = 2.6$. The log-log plot in Fig. 2(a) reveals that τ_M in WHAM scales as $\tau_M \sim M^{2.3}$ for large M regardless of the value of δ_Z . In contrast, τ_M in ST-WHAM is independent of M , because the need to determine Z_α has been eliminated.

The main source of error in finite length simulations is the statistical fluctuation of H_α . The accuracy of WHAM and ST-WHAM, is compared by plotting $\epsilon(\beta_S)$ and $\epsilon(S)$ as a function of MC steps per spin (MCS) in Figs. 2(b) and 2(c), respectively, for canonical runs at evenly distributed temperatures with $M = 4$. All quantities are averages over ten independent realizations and $\tilde{\beta}_S$ is calculated from the reweighted \tilde{H}_α . Both $\epsilon(\tilde{\beta}_S)$ and $\epsilon(\tilde{S})$ in WHAM depend strongly on δ_Z and gradually decrease with decreasing δ_Z . These errors reach the accuracy of ST-WHAM for $\delta_Z = 10^{-11}$, implying that

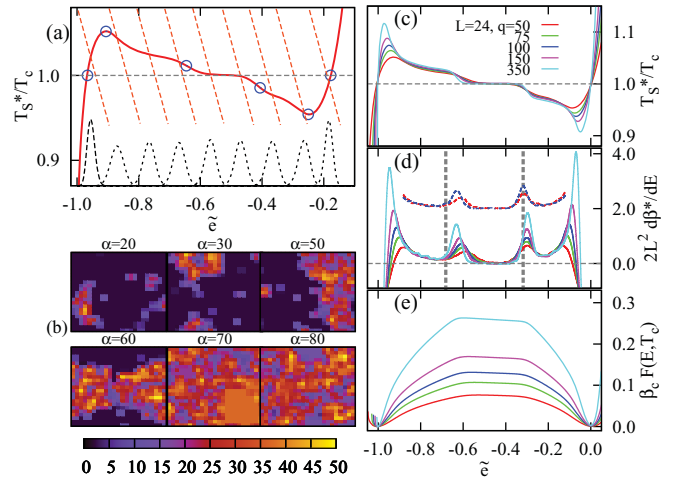


FIG. 3. Results for the q -state 2D Potts model. (a) T_α^{eff} (dashed line), T_S^* (solid line), H_α (dotted line), and characteristic energies \tilde{e}_0 , $\tilde{e}_{s,1}$, $\tilde{e}_{ds,2}$, $\tilde{e}_{ds,1}$, $\tilde{e}_{s,2}$, and \tilde{e}_d (see the text) from left to right (circles); (b) representative configurations at different α for $q = 50$ and $L = 24$, (c) $T_S^*(\tilde{e})$, (d) $\beta_S^*(\tilde{e})$, (e) free energy densities per spin $F(\tilde{e}, T_c)$ with varying q . In (a), $\alpha = 10, 20, 30, 40, 50, 60, 70, 80$, and 90 in both T_α^{eff} and H_α . The same color scheme is applied to (c)–(e).

ST-WHAM corresponds to the asymptotic limit of WHAM associated with $\delta_Z = 0$. Because $\epsilon(S^*)$ is greater than the error intrinsic to the mapping ($\approx 10^{-9}$), the errors in S^* are mostly due to the statistical uncertainties in H_α .

In addition to the simplification of the numerical analysis realized using ST-WHAM, the direct determination of β_S via ST-WHAM unveils key signatures characteristic of phase transitions.⁹ Of particular interest is its use with the generalized ensemble weight,

$$W_\alpha = [\lambda_\alpha + \gamma(E - \mathcal{E})]^{-1/\gamma}, \quad (11)$$

where $\{\lambda_\alpha, \gamma, \mathcal{E}\}$ are a set of tunable parameters.^{12,13} This form of W_α yields $H_\alpha \approx \exp\{\kappa^*/2(E - E_\alpha^*)^2\}$ centered at the crossing point E_α^* between T_S and $T_\alpha^{\text{eff}} = [\partial w_\alpha / \partial E]^{-1} = \lambda_\alpha + \gamma(E - \mathcal{E})$. Here $\kappa^* = (\gamma - \gamma_S)/T_S^2(E_\alpha^*)$ and $\gamma_S = T_S'(E_\alpha^*)$. If we vary γ from $-\infty$ to γ_S , we can continuously tune the ensemble from $\delta(E - E_\alpha^*)$ to a locally flat H_α . The use of W_α is particularly well suited to sampling strong first-order phase transitions, in which coexisting states are associated with the characteristic backbending of T_S , i.e., $\gamma_S(E) < 0$.⁹ Phase-mixed configurations are intrinsically unstable in the canonical ensemble due to $\kappa^* > 0$. These metastable states are directly accessible in W_α with $\gamma < \gamma_S$ via a unimodal H_α .¹³

To explore the synergistic combination of ST-WHAM with generalized ensembles in strong first-order phase transitions, we consider the q -state 2D Potts model with toroidal geometry. For each q , two short canonical runs at $T_l = 0.9T_c$ and $T_h = 1.1T_c$, with $T_c = 1/\ln(1 + \sqrt{q})$ the critical temperature of the infinite lattice, were performed to approximately determine the internal energies E_l and E_h , giving $\gamma = 10(T_h - T_l)/(E_l - E_h) < \gamma_S$ for all sampled energies and $\mathcal{E} = E_l$, $\lambda_1 = T_l$, $\lambda_M = T_h + \gamma(U_h - U_l)$, and $\lambda_\alpha = \lambda_1 + (\alpha - 1)(\lambda_M - \lambda_1)/(M - 1)$.¹³ Runs of 10^6 MCS for each α with $M = 100$ associated with T_α^{eff} in Fig. 3(a) produce

successive unimodal H_α , which are merged to determine T_S^* for $q = 50$. Note that H_α are peaked at crossing points E_α^* between T_α^{eff} and T_S^* . Representative configurations at intermediate α in Fig. 3(b) demonstrate that various mixed-phase configurations are sampled.

The non-monotonic variation of T_S^* in Fig. 3(a) characterizes a sequence of phase transitions.¹⁴ The local maximum and minimum at $\tilde{e}_{s,1}$ and $\tilde{e}_{s,2}$ are associated with the nucleation of disordered ($\alpha = 20$) and ordered ($\alpha = 80$) droplets in each stable phase. The flat region near T_c between $\tilde{e}_{ds,1}$ and $\tilde{e}_{ds,2}$ ($> \tilde{e}_{ds,1}$) represents the formation of strip phases corresponding to $\alpha = 50$ and 60 in Fig. 3(b). Here $\tilde{e} = (e - e_o)/(e_o - e_d)$, with e_o and e_d the energies of the free energy minima of the ordered and disordered phases at T_c . As q increases both backbending ($\tilde{e}_{s,1} < \tilde{e} < \tilde{e}_{s,2}$) and the strip phase region ($\tilde{e}_{ds,1} < \tilde{e} < \tilde{e}_{ds,2}$) gradually expand with more pronounced transition markers [see Fig. 3(c)].

All the relevant transitions are determined by identifying the locations of zeros and peaks in the derivatives of β_S^* in Fig. 3(d). The two central peaks at $\tilde{e}_{ds,1}$ and $\tilde{e}_{ds,2}$, locate the transitions between the droplet and strip phases, and are close to the droplet-strip transition energies (gray vertical lines) in the infinite volume limit, $\pi^{-1} - 1$ and π^{-1} , respectively.¹⁵ For L increasing from 24 to 36 (dashed line) both $\tilde{e}_{ds,1}$ and $\tilde{e}_{ds,2}$ for $q = 50$ and 100 shift to the thermodynamic transition points. Zeros of β_S^* corresponding to $\tilde{e}_{s,1}$ and $\tilde{e}_{s,2}$ yield “effective spinodal points,” in which metastable droplets start to grow by absorbing background fluctuations in stable phases.¹⁴ The free energy densities per spin in Fig. 3(e), $F(\tilde{e}, T_c) = \tilde{e} - T_c S^*/2L^2$, exhibit wells at $\tilde{e} = -1$ and 0 , and inflections at $\tilde{e}_{s,1}$ and $\tilde{e}_{s,2}$, with flat humps between $\tilde{e}_{ds,1}$ and $\tilde{e}_{ds,2}$. Here F is set to zero at \tilde{e}_d .

In summary, an efficient weighted histogram analysis method, ST-WHAM, has been proposed in terms of intensive variables. The method directly determines β_S and S with no iterative evaluations of partition functions, providing the same accuracy as conventional WHAM for infinite iterations. If combined with parameterized, generalized ensemble weights, ST-WHAM gives the complete sequence of phase transitions among various metastable states via distinct markers in β_S as exemplified by our simulations of the q -state Potts model. We anticipate that directly accessing both β_S and S “on the fly” during the simulation via ST-WHAM will allow for considerable acceleration in the performance of sampling algo-

ri thms that rely on iterative refinements of S (Ref. 16) or β_S .¹⁷

In closing, some potential limitations in our approach should be addressed. As both WHAM and ST-WHAM assume overlaps between energy distributions extra interpolations or extrapolations of $H_\alpha(E)$ using a proper functional form would be necessary for unvisited energy regions in rugged or glassy systems. The numerical instability of computing partial derivatives with respect to each order parameter and recovering extensive quantities from intensive ones poses a challenge in the extension of our approach to PMF calculations in multiple order parameters.

We thank the National Science Foundation (NSF) (CHE-0750309, CHE-1114676, and CHE-0833605) and the National of Institutes of Health (NIH) (R01 GM076688) for support. Special thanks to Professor Harvey Gould for a careful reading of the manuscript.

- ¹A. M. Ferrenberg and R. H. Swendsen, *Phys. Rev. Lett.* **63**, 1195 (1989).
- ²M. E. J. Newman and G. T. Barkema, *Monte Carlo Methods in Statistical Physics* (Clarendon, Oxford, 1999).
- ³D. Frenkel and B. Smit, *Understanding Molecular Simulation: From Algorithms to Applications* (Academic, San Diego, 1996).
- ⁴S. Kumar, D. Bouzuda, R. H. Swendsen, P. A. Kollman, and J. M. Rosenberg, *J. Comput. Chem.* **13**, 1011 (1992).
- ⁵M. Souaille and B. Roux, *Comput. Phys. Commun.* **135**, 40 (2001).
- ⁶J. Kastner and W. Thiel, *J. Chem. Phys.* **123**, 144104 (2005).
- ⁷J. D. Chodera, W. C. Swope, J. W. Pitera, C. Seok, and K. A. Dill, *J. Chem. Theory Comput.* **3**, 26 (2007).
- ⁸T. Berau and R. H. Swendsen, *Comput. Phys. Commun.* **228**, 6119 (2009).
- ⁹D. H. E. Gross, *Rep. Prog. Phys.* **53**, 605 (1990); D. J. Wales and R. S. Berry, *Phys. Rev. Lett.* **73**, 2875 (1994); J. Kim, T. Keyes, and J. E. Straub, *Phys. Rev. E* **79**, 030902(R) (2009).
- ¹⁰J. Kim, Y. Fukunishi, and H. Nakamura, *J. Chem. Phys.* **121**, 1626 (2004); J. Kim, Y. Fukunishi, A. Kidera, and H. Nakamura, *ibid.* **121**, 5590 (2004).
- ¹¹P. D. Beale, *Phys. Rev. Lett.* **76**, 78 (1996).
- ¹²C. Tsallis, *J. Stat. Phys.* **52**, 479 (1988).
- ¹³J. Kim, T. Keyes, and J. E. Straub, *J. Chem. Phys.* **132**, 224107 (2010); J. Kim and J. E. Straub, *ibid.* **133**, 154101 (2010).
- ¹⁴L. G. MacDowell, P. Virnau, M. Muller, and K. Binder, *J. Chem. Phys.* **120**, 5293 (2004).
- ¹⁵B. Bauer, E. Gull, S. Trebst, M. Troyer, and D. A. Huse, *J. Stat. Mech.* P01020 (2010).
- ¹⁶B. A. Berg and T. Celik, *Phys. Rev. Lett.* **69**, 2292 (1992).
- ¹⁷U. H. E. Hansmann, Y. Okamoto, and F. Eisenmenger, *Chem. Phys. Lett.* **259**, 321 (1996); N. Nakajima, H. Nakamura, and A. Kidera, *J. Phys. Chem. B* **101**, 817 (1997); J. Kim, Y. Fukunishi, and H. Nakamura, *Phys. Rev. E* **70**, 057103 (2004).